Ball Indentation Analysis of a Tough Polymer Sheet

Malik M. Nazeer, M. Afzal Khan, A. Naeem, and A. ul Haq

(Submitted 22 January 2001)

The ball indentation process of tough polymer sheet clamped at its periphery has various particular response characteristics. These characteristics of the polymer sheet have been discussed in comparison to the ductile metal sheet undergoing a similar indentation process. The ball indentation process of polymer sheet is also mathematically analyzed to evaluate fracture toughness and distribution of the energy used. This analysis is useful for designers to foresee the pre- and post-peak load response and possible aftermath. The information and results presented may be useful to meet some particular design and utility demands. Data for a number of tests was recorded and analyzed and it was observed that at a particular load and corresponding displacement, fracture first begins within the dimple. The fracture toughness and energy used were calculated using a mathematical model developed for computations. The energy-based equations of Rigid-Plastic Fracture Mechanics have been used for computational model for steel balls indentation, perforation, and fracture propagation. The dependence of various parameters on the indenting ball diameter and bearing of the anisotropy due to sheet extrusion is elaborated.

Keywords elasto-plastic flow, fracture propagation, fracture toughness, perforation, polymer indentation characteristics

1. Introduction

The ball indentation in a tough polymer sheet is a complex process, not just bulging of ductile metal sheets (multi-axial stretching).[1] In ductile metal sheets, the bending deformation in elastic and plastic zones of the material is accompanied by shear and plastic flow deformation leading to dimple formation, necking and fracture along the necking line and then along with radial crack initiation and propagation which results in petal formation.[2,3] In polymers, the process is distinct from ductile metal sheets, both in pre- and post-crack initiation and the difference is clearly visible, both in specimen appearance and response plots. The process in tough polymer is elastic deformation dominated even in the pre-fracture zone. In the post-fracture zone, the process is again purely elastic, contrary to ductile metals where it is pure plastic.

The energy based equation for rigid-plastic fracture mechanics used in the incremental plastic work per unit volume and fracture work according to Griffith[4] is given by:

$$Xdu = d\wedge + RdA + d\Gamma$$

It was discussed and applied by Atkins et al.[5] for independent measurement of R in monolithic materials undergoing elasto-plastic flow and fracture in metal sheets. In metal sheets analysis, the term $d\wedge$ related to elastic strain energy is neglected due to its small effect on the resulting large plastic deformation,[3,6-10] whereas it is retained in quasi-elastic fracture of bodies behaving in an elastic manner. The term $d\Gamma$ represents the extensive remote flow irreversibly accompanying crack propagation. In the study and formulation for this process in ductile metal sheet carried out by Khan et al.[3] and

Malik M. Nazeer, M. Afzal Khan, A. Naeem, and **A. ul Haq,** Dr. A.Q. Khan Research Laboratories, P.O. Box 502, Rawalpindi, Pakistan. Contact e-mail: mmnazeer@inst-rd.isb.sdnpk.org.

Nomenclature

A	crack area
E	Young's modulus of elasticity
F	applied force
$2H_2$	major crack length
N_p	number of cracks
R	fracture toughness
u	displacement
$\wedge$	elastic strain energy
τ	plastic strain energy
W_T	total work input during indentation process
W_B	work input before the peak load
W_F	work input after the peak load
W_f	fracture work for petal formation
W_E	work required for elastic deformation of specimen outside the dimple.
W_e	work required for deformation of the specimen portion outside the dimple after passing the peak load position
X	load
r_p	radius of specimen held within the die
r_b	radius of indenting ball
r_d	radius of dimple face of the specimen under direct ball contact at the peak load
t_0	initial sheet thickness
t_f	final average sheet thickness in the ball indentation zone
x_0	width of sheet ring outside the ball indentation zone
z	distance of a fiber from the neutral surface in bending process
σ	stress
δ	ball displacement under compression load
δ_p	ball displacement at peak load
δ_s	displacement at the ball slip-drop position

Nazeer et al.[7,8] the term d∧ was neglected and $d\Gamma$ was retained. Thus the equation used was $Xdu = RdA + d\Gamma$.

In the case of tough polymer sheets, however, the converse is true—both pre- and post-fracture zones and hence their formulation differs. In the ball indentation of tough polymer sheets, the radial cracks precede necking which is contrary to the metal sheet indentation.[3] Moreover, the crack initiation is in stages to give way to the ball compared with metal sheet where these stages are not found in the process. The term $d\wedge$ in tough polymer sheets analysis case is not negligible whereas in ductile metal sheets it has very little effect on the results. The term $d\Gamma$ used in the plastic deformation has no bearing after the crack initiation because after the crack initiation, the elastic deformation is regained in place of plastic flow, which is not observed in case of ductile metal sheets. Thus for the case of post cracks, the initiation analysis equation becomes:

$$Xdu = d\wedge + RdA$$

The tough polymer (polycarbonate) has elastic modulus of 2.4 GPa, tensile strength 55-69 MPa, and fracture toughness 2.75-3.3 MPa/m. Its sheet is amorphous and does not craze readily at room temperature. Its fracture toughness has excellent fatigue behavior and has a low frequency sensitivity factor during fatigue crack propagation testing.[11] For response of residual stresses and dimensional stability, Ref. 6 is a valuable contribution on the subject.

2. Experiment

The tough polymer (polycarbonate) sheet samples, prepared through ram extrusion and continuous compression molding process[12] clamped around the periphery, were indented with steel balls of different diameters from 6-12 mm, using an Instron Testing Machine. The samples perforation involved elastic and plastic deformation, crack initiation and propagation, and finally the material perforation. The fracture process is completed rapidly and the applied load dropped along with completion of elasto-plastic deformation of the tough polymer.

The Universal Instron Testing Machine with 10 KN load capacity [Model No. 1195] was used with a quasi-static compression load applied to the 90 mm diameter tough polymer sheet samples. A die with 63 mm internal diameter was used to tightly hold the discs with 6 M10 bolts (Fig. 1). The hard steel balls were fixed in an assembly for indentation of the tough polymer sheet. The speed of the indenting ball in this experiment was 6×10^{-6} m/s. An optical microscope was used to record the morphology of the fracture surfaces. Steel balls of 6, 8, 10, and 12 mm diameters were used in this experiment for indentation of 1.5 mm thick tough polymer extruded sheet.

3. Different Indentation Stages

The elasto-plastic behavior and load versus displacement diagram of the tough polymer sheet indented with a steel ball is shown in Fig. 2. From O to A the displacement of the ball is linear and the sheet is in elastic deformation zone. From A to B, the deformation in the central portion of the plate starts entering into plastic zone, while the peripheral portion outside the dimple is still in the elastic range. From B to C the load is increasing, circular dimples start forming, and a crack initiates from C to D. From D to F the crack propagates across the dimple and there is an almost sudden drop in resistance to the applied load and the line is linear at this stage. Up to F, there is only one radial crack propagating on both sides outside the dimple. Finally, from F to G one or two more radial cracks within the dimple at 90° to the previous main crack takes place, which is preceded by elastic deformation. The ball indentation process ends at G, when the ball drops through the perforated sheet. Thus the process is completed and the specimen is relieved of the elastic deformation. Figure 3 shows the photograph of a perforated specimen.

4. Fracture Toughness Analysis

The total work W_T, work input till peak load (maximum) position W_B, and work after peak load W_F (Fig. 4) are function of ball radii and are calculated by integration of load displacement diagrams (Fig. 5). The details of the indentation parameters and indentation ball and the specimen radii used in the analysis are shown in Fig. 6 and 7. In this experiment, the interest was to find the fracture toughness of this material based on the work input after the peak load and the cracks developed along the radial direction. After the crack initiation, the load drops suddenly, and crack propagates radially, the elastic deformation takes place in the peripheral zone outside the central area, where a pre-peak load plastically deformed dimple has already been formed in the sample. The specimen is partly relieved of the stresses due to creation of one radial crack and the further crack propagation is accompanied by the elastic deformation in the material. There is no sign of plastic deformation after the major crack initiation as the specimen regains its shape with cracks across the pre-crack initiation plastically formed dimple. There is no plastic bending of the petals as in the case of a ductile metal sheet specimen.[3] The work input W_F after the peak load is the sum of the fracture work W_f and elastic deformation work W_e:

$$W_F = W_f + W_e \quad \text{(Eq 1)}$$

At the crack initiation stage only one major crack is produced across the dimple, which is perpendicular to the extrusion direction of the specimen. This big crack is large enough to cross the boundaries of the dimple and goes to the end of periphery of the specimen in the die. One or two small cracks are also formed at 90° to the major crack to give way to the ball to fall down. The subsequent cracks do not go beyond the dimple boundaries, and stay within the ball radius. The thickness of the sheet within the dimple is reduced to t_f whereas in the outside peripheral area, it does not change. Therefore, the fracture work is given by:

$$W_f = N_p r_b t_f R + 2(H_2 - r_b) t_0 R \quad \text{(Eq 2)}$$

N_p is the number of cracks produced, which are the major ones considering it to be two each initially from the center to the periphery and the other as two small one propagating in right angles to the major crack.

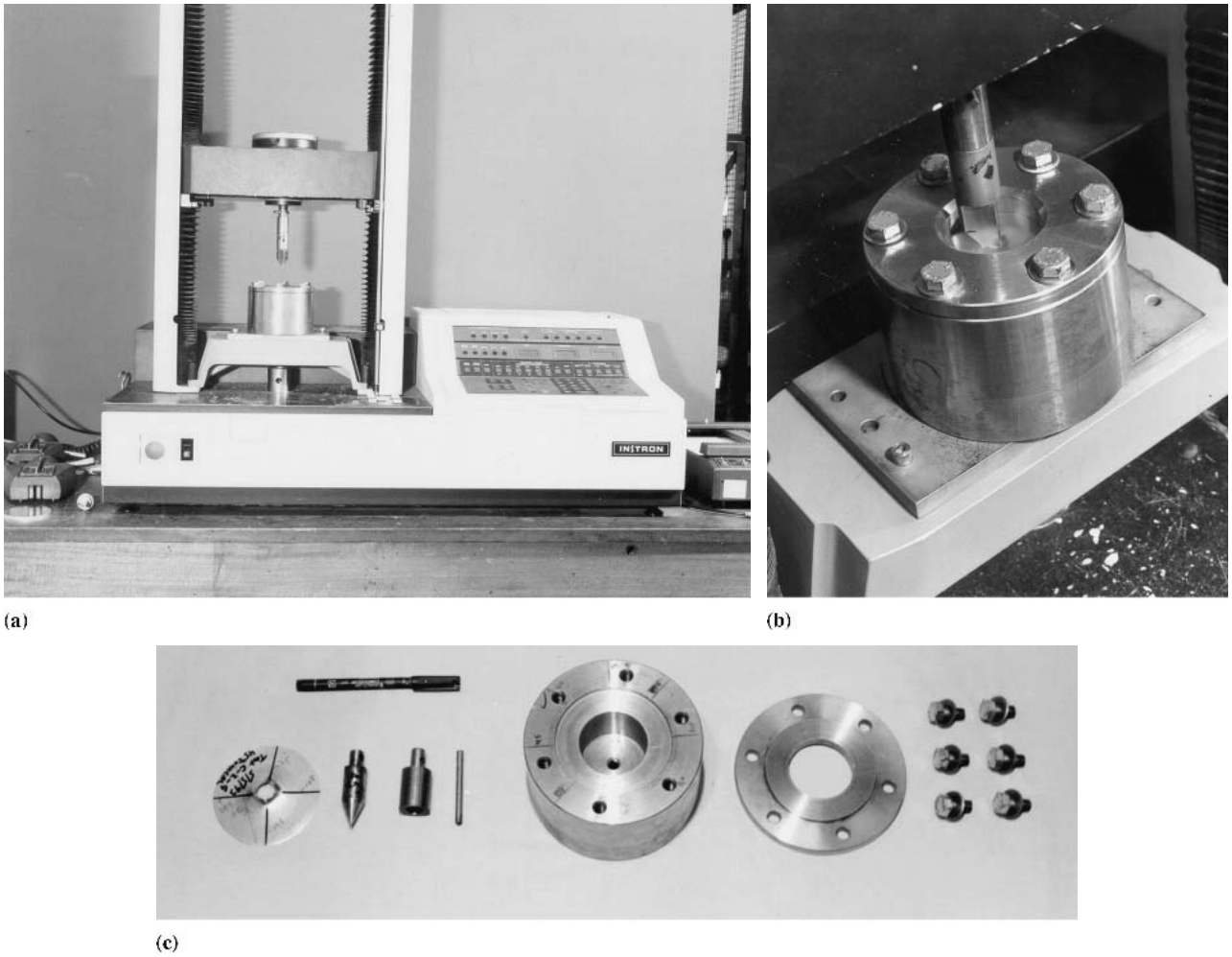

Fig. 1 Ball indentation experiment on Instron machine-specimen, die, cap, bolts, and ball assembly

After the crack initiation, the specimen is relieved of a central constraint and is nearly like a cantilever with a fixed base end equal to $2\pi r_p$ and loaded at the tip by the point load F equal to the total load. The bending moment M_r and the second moment of the cross-sectional area I_r at a distance r from the center[13,14] are given by:

$$M_r = Fr$$

$$I_r = \frac{2\pi r t_0^3}{12} = \frac{\pi r t_0^3}{6}$$

Also

$$\frac{\sigma}{z} = \frac{M_r}{I_r}$$

Thus

$$\sigma = \frac{6Frz}{\pi r t_0^3} = \frac{6Fz}{\pi t_0^3}$$

The total elastic work[15] is therefore given by:

$$dW_E = \int \sigma \varepsilon dV = \int \frac{\sigma^2 dV}{E} = \frac{\pi r_p^2}{E} \int_{-t_0/2}^{t_0/2} \sigma^2 dz = \frac{36F^2 r_p^2}{\pi t_0^6 E} \int_{-t_0/2}^{t_0/2} z^2 dz$$

Thus

$$W_E = \frac{3F^2 r_p^2}{\pi t_0^3 E}$$

The elastic work is stored in the form of energy into the circular area of the ring outside the dimple, thus:

$$W_E = \frac{3F^2}{\pi t_0^3 E}(r_p^2 - r_d^2)$$

W_E is the total elastic energy stored in the ring around the ball dimple, to the state when the ball starts slipping out and

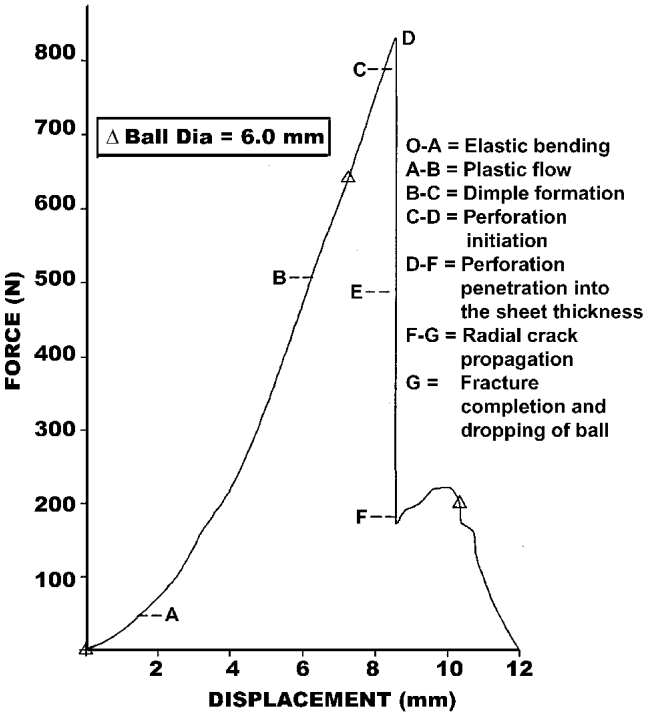

Fig. 2 The material behavior at various stages in steel ball indentation of 16 gauge tough polymer sheet

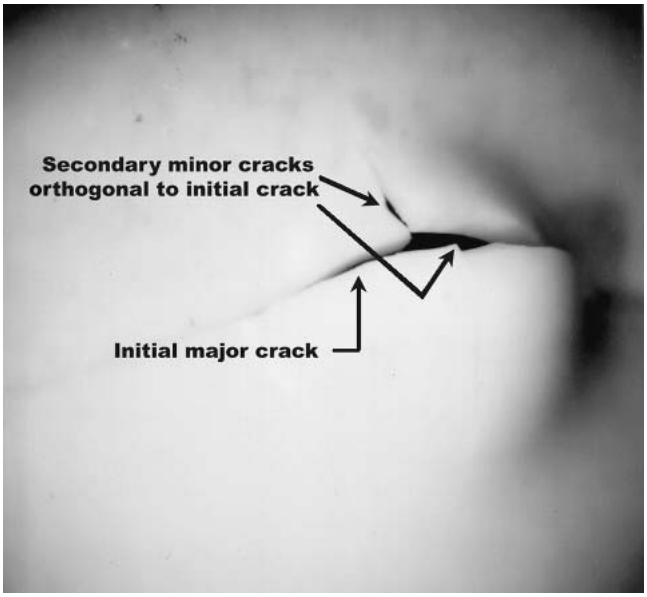

Fig. 3 12 mm diameter ball indentation in 16 gauge (1.5 mm) tough polymer (polycarbonate) sheet

drops through the hole (i.e., maximum load position during fracture propagation stage). The part of the elastic energy stored in the specimen after the crack initiation is thus given by:

$$W_e = \frac{W_E}{\delta_s}(\delta_s - \delta_p)$$

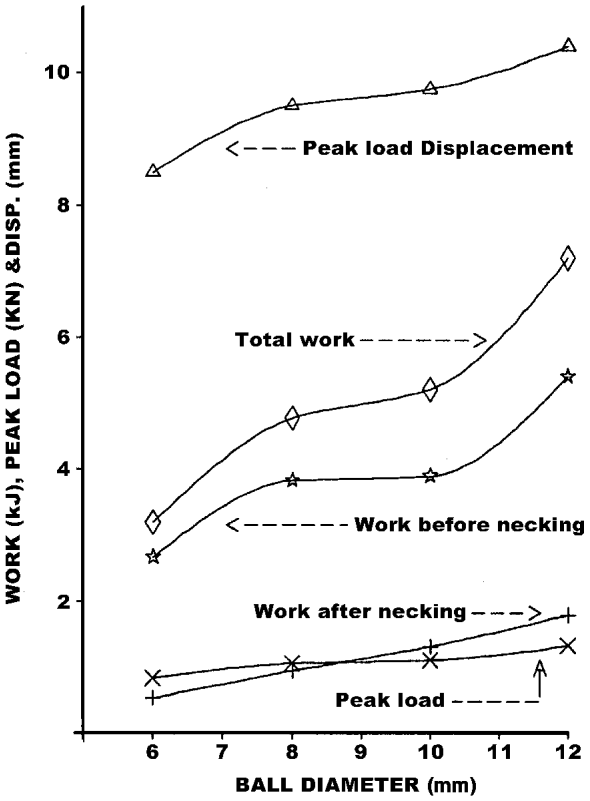

Fig. 4 Work input, max. load, and peak load displacement versus ball diameter

Or

$$W_e = \frac{3F^2 r_p^2}{\pi t_0^3 E \delta_s}(r_p^2 - r_d^2)(\delta_s - \delta_p) \quad \text{(Eq 3)}$$

knowing W_e from Eq 3 the fracture toughness is given by:

$$R = \frac{W_F - W_e}{t_f N_p r_b + 2(H_2 - r_b)t_0} \quad \text{(Eq 4)}$$

And in case of known fracture toughness the number of cracks are given by:

$$N_p = \frac{1}{t_f r_b}\left[\frac{W_F - W_e}{R} - 2(H_2 - r_b)t_0\right] \quad \text{(Eq 5)}$$

W_F is calculated by integration of the load displacement diagrams (Fig. 5) and used in the above equations. The results of the above analysis are given in Table 1 and 2. The cracks were radially propagated and were dependent on the sheet extrusion processing direction.

5. Results and Discussion

Figure 5 shows the response of load versus displacement for various indenting balls. The increase in load with the increase

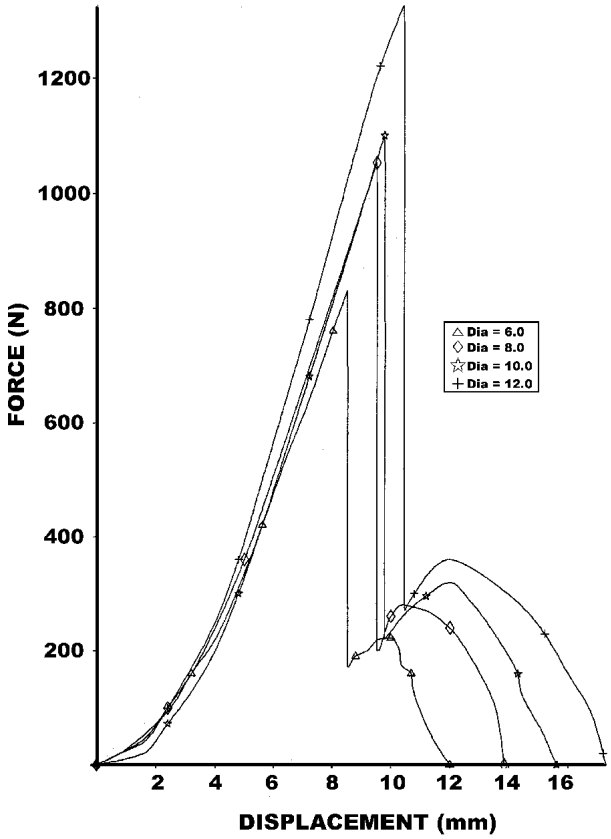

Fig. 5 Load displacement for 6, 8, 10, and 12 mm diameter ball indentation in 16 gauge tough polymer sheet

in ball diameter along with peak load and peak load displacement is significant and systematic as the last two rise exponentially. Also, response after the crack initiation is dependent on indenting ball diameter, and is systematic. The decreasing load line drops rapidly from peak position to a point and then it jumps upward and gradually comes down to the baseline. This second curve creation is a unique phenomenon for this material.

The work input before crack initiation versus displacement is shown in Fig. 8 for 1.5 mm thick tough polymer sheet obtained by incremental integration of the load displacement diagrams (Fig. 5). This gives the work input up until the peak load (maximum) for indenting steel balls of different diameters. The work input increases systematically with the displacement and the ball diameters except an abnormal prolonged fracture initiation in case of ball of 8 mm diameter perhaps due to some local abnormality. Figure 9 shows the work input versus the ball displacement for different balls after the crack initiation. This gives the work input by different balls for elastic bending, and crack propagation. The figures show that crack initiation displacement, total post-crack initiation work, and ball drop displacement are all systematically ball diameter dependent. Figure 10 gives the total work input versus ball displacement during the indentation process. This is the combined response of Fig. 8 and 9. The sharp bend in the curve profile at the crack initiation point shows the difference in slope around that point. The slope of the curve beyond this

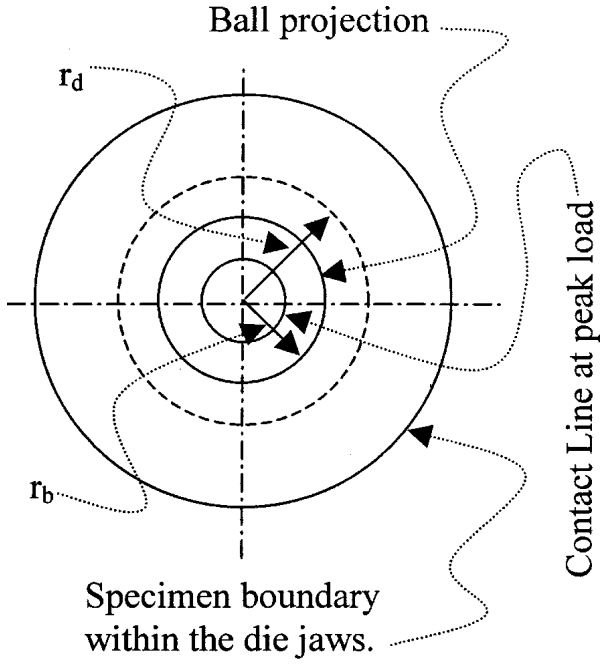

Fig. 6 Specimen and ball diameters along with specimen and ball contact line at peak load

point indicates its elastic response with minute difference in its slope compared with that at the very beginning stage perhaps due to plastic hardening and variation in the sheet thickness within the dimple.

Table 1 shows the dependence of number of cracks dimple diameter, major crack length, and final thickness dependence on the indenting ball diameter. Major crack length decreases while all the other parameters increase with indenting ball di-

Table 1 Experimentally Observed Results of Ball Indentation in Tough Polymer Sheet

Ball Dia., mm	No. of Cracks	Dimple Diameter, mm	Final Thickness, mm	Major Crack Length, mm	Crack Angles (deg.) w. r. t. Sheet Extrusion Direction
6	3	6.64	1.08	24.0	120, 200, 300
8	4	8.82	1.12	24.0	5, 95, 182, 275
10	4	11.85	1.16	23.5	0, 85, 182, 265
12	4	12.40	1.22	23.2	45, 135, 285, 305

Table 2 The Computed Results of Ball Indentation in Tough Polymer Sheet

Ball Dia., mm	W_T	W_B	W_F	W_e	W_f	R, kJ/m^2
6	3.1978	2.6673	0.5305	0.2442	0.1863	3.94
8	4.7651	3.8258	0.9393	0.6348	0.3.45	3.91
10	5.2077	3.8954	1.3123	0.9831	0.3292	4.18
12	7.1891	5.4024	1.7867	1.4499	0.3368	4.16

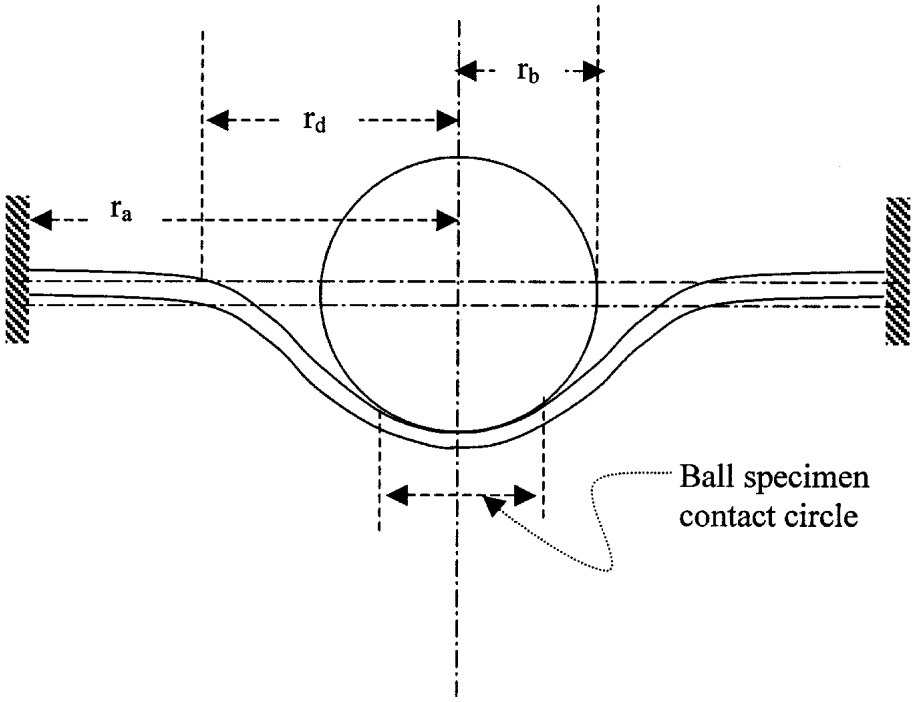

Fig. 7 Sketch showing ball indentation parameters

ameter. The crack angles show their dependence on the sheet extrusion direction (i.e., major crack always normal and two subsequent smaller cracks in the sheet extrusion direction). This, however, is independent of indenting ball diameter.

Table 2 and Fig. 4 show the resulting peak load, peak load displacement, total work input, work input till peak load position, and work input after peak load until the end of perforation versus indenting ball diameter. The ball diameter was directly related to the material plastic flow within the die. The total work W_T, work input till peak (maximum) load position W_B, and work after peak load W_F are a function of ball radii (Fig. 4) and calculated by integration of load displacement diagram (Fig. 5). All of the work inputs and the peak load displacements increase exponentially with the increase in indenting ball diameter.

6. Conclusions

1) The mathematical model can be applied for calculations of fracture toughness of tough polymer sheets with energy-based equations, using load-displacement diagrams obtained during steel ball indentation and perforation.
2) The crack angles after the perforation with steel balls gave the orientation against the 1.5 mm sheet's extrusion processing direction and followed systematic behavior (i.e., cracks were significantly affected by anisotropy). The major crack is almost 90° to the sheet extrusion processing direction followed by two small cracks perpendicular to the larger crack. This is different than that for the ductile metals sheets.
3) The work input, crack initiation, and ball displacements

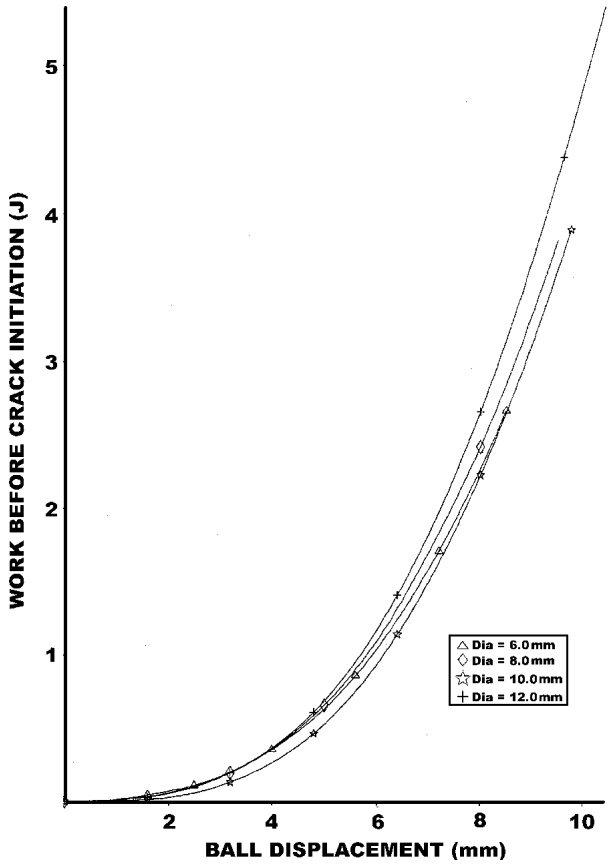

Fig. 8 Work before crack initiation versus ball displacement in tough polymer indentation

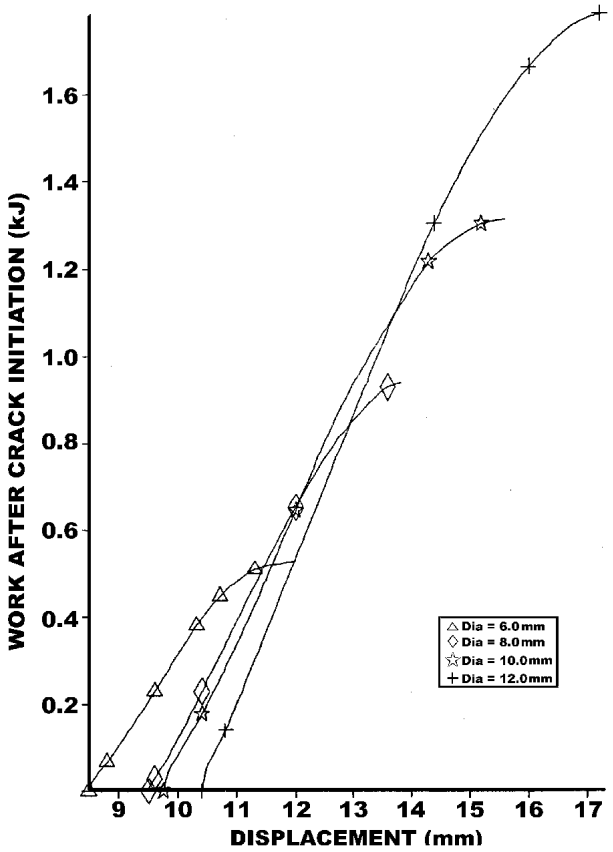

Fig. 9 Work after crack initiation versus steel ball displacement in 16 gauge tough polymer sheets

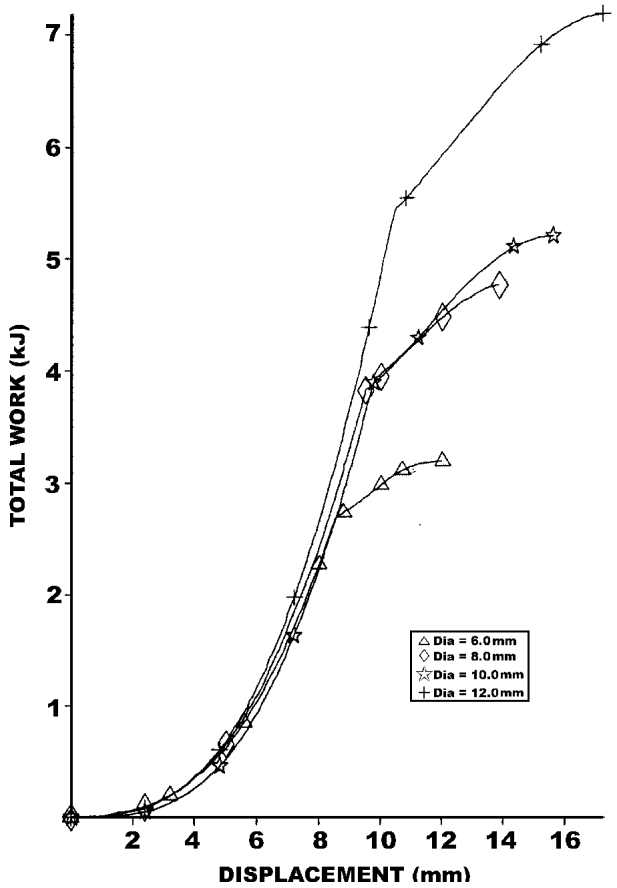

Fig. 10 Total work input versus steel ball displacement in 16 gauge tough polymer sheet indentation

are exponentially ball diameter dependent (i.e., these all increased exponentially with the indenting ball diameter).

4) The crack propagation process is accompanied by elastic deformation of the polymer material in contrast to the response of metal sheet response, which is accompanied by the plastic deformation.
5) The pre-crack initiation stage is dominated by elastic deformation, in contrast to metal sheet response which is dominated by plastic deformation.
6) There is one major crack, which propagates in both directions, and one or two subsequent small cracks with tandem initiation contrary to the metal sheet response, where almost all of the cracks initiate simultaneously out of which a few die down at initial stages while most of them propagate radially.
7) Petals and lip formation, a characteristic phenomenon of ball indentation in ductile metal sheets, was absent in this experiment on tough polymer sheet. This material regains its pre-crack initiation shape without load, with only addition of cracks.
8) The necking and fracture along the necking line in tough polymer sheets were not observed in this experiment.
9) The dependence of various parameters directly related to the steel balls diameter in this indentation process were different from the results obtained on the similar process in the metal sheet.
10) The number of cracks, dimple diameter, and final sheet thickness increase with the ball diameter while major crack length decreases with it.

Acknowledgments

The authors are highly thankful to Professor Dr. A.G. Atkins, Department of Engineering, Reading University, Reading, UK, for his useful discussions on this topic and his continuous guidance extended both, directly and indirectly over many years. The authors also thank Mr. Muhammad Yousaf Malik for his help in typesetting this manuscript.

References

1. T. Wierzbicki and N. Jones: *Fracture*, John Wiley, New York, NY, 1988, pp. 107-32.
2. F.A. McClintock: "A Criterion for Ductile Fracture by the Growth of Holes," *J. Appl. Mech.,* 1968, *35*, pp. 363-71.
3. M.A. Khan, M.M. Nazeer, A. Naeem, A. ul Haq, and A.G. Atkins: "Computer Modeling of Elasto-Plastic Fracture Mechanics of Ball Indentation in Ductile Aluminum Sheet" in *Proc. EUROMAT 95,* Padua/Venice, Italy, 1995, pp. 491-94.
4. A.G. Atkins and Y.W. Mai: *Elastic and Plastic Fracture*, Ellis Harwood, John Wiley, UK, 1988, pp. 574-80.
5. A.G. Atkins: "On Cropping and Related Processes," *Int. J. Mech. Sci.,* 1980, *22,* pp. 215-31.
6. K. Vijay and G.E. Stokes: "Residual Stresses and Dimensional Stability in Injection Molded Thermoplastic Parts" in *Proc. Symposium on Long Term Performance Issue in Polymer Chemistry and Physics,*

Corporate Research & Development, Schenectady, NY, 28 Nov.-1 Dec., 1995.
7. M.M. Nazeer, M.A. Khan, A. Naeem, and A. ul Haq: "Analysis of Conical Tool Perforation of Ductile Metal Sheets," *Int. J. Mech. Sci.,* 2000, *42*, pp. 1391-403.
8. M.M. Nazeer, M.A. Khan, A. Naeem, A. ul Haq, and A.G. Atkins: "Mathematical Analysis of Sharp Tool Indented Aluminium Sheet Curvature" in *Proc. Int. Conf. on Pure and Applied Mathematics,* ICPAM 95, Bahrain, 1995.
9. A.G. Atkins, M.A. Khan, and J.M. Liu: "Necking and Radial Crack Around Perforation in the Sheet at Normal Incidence," *Int. J. Impact Eng.,* 1998, *21*(7), pp. 521-39.
10. M.M. Nazeer, M.A. Khan, A. Naeem, and A. ul Haq: "Response of Ductile Metal Sheet Parameters to the Cone Angle of Indenting Conical Tool," *Int. J. Mater. Perform.,* 2000.
11. R.W. Hertzberg: *Deformation and Fracture Mechanics of Engineering Materials,* John Wiley and Sons, New York, NY, 1976.
12. A.B. Strong: "Plastic Materials and Processing," 2nd ed., Prentice Hall, NJ, 2000, pp. 244-86 and 640-748.
13. G.H. Ryder: "Strength of Material," English Language Book Society and McMillan Press Ltd, London, UK, 1996, pp. 86-128.
14. S. Timoshenko: "Strength of Material – Part I Elementary," Van Nostrand Reinhold, New York, NY, pp. 415-28.
15. S. Timoshenko: "Strength of Material – Part II Advanced Theory and Problems," 3rd ed., CBS Publishers and Distributors, Delhi, India, 1986, p. 448.